

Journal of Materials Chemistry A

Accepted Manuscript



This is an *Accepted Manuscript*, which has been through the Royal Society of Chemistry peer review process and has been accepted for publication.

Accepted Manuscripts are published online shortly after acceptance, before technical editing, formatting and proof reading. Using this free service, authors can make their results available to the community, in citable form, before we publish the edited article. We will replace this *Accepted Manuscript* with the edited and formatted *Advance Article* as soon as it is available.

You can find more information about *Accepted Manuscripts* in the [Information for Authors](#).

Please note that technical editing may introduce minor changes to the text and/or graphics, which may alter content. The journal's standard [Terms & Conditions](#) and the [Ethical guidelines](#) still apply. In no event shall the Royal Society of Chemistry be held responsible for any errors or omissions in this *Accepted Manuscript* or any consequences arising from the use of any information it contains.



Journal Name

ARTICLE

FeCl₃ Intercalated Few-Layer Graphene for High Lithium-Ion Storage Performance

Xin Qi, Jin Qu, Hao-Bin Zhang*, Dongzhi Yang, Yunhua Yu, Cheng Chi and Zhong-Zhen Yu*

Received 00th January 20xx,
Accepted 00th January 20xx

DOI: 10.1039/x0xx00000x

www.rsc.org/

We report a facile and efficient approach to prepare graphene and FeCl₃-intercalated few-layer graphene (FeCl₃-FLG) with stage 1 FeCl₃-graphite intercalation compounds (GICs) as the precursor by a non-oxidation process. The enlarged interlayer spacing by the intercalation of FeCl₃ greatly weakens the interaction among graphite sheets and thus facilitates the exfoliation of FeCl₃-GICs. By ultrasonic treatment, FeCl₃-GICs are well exfoliated to graphene sheets (<2 nm) with a high yield of 100%, while the ultrasonication of pristine graphite is less efficient with a low yield (about 32%) of graphene sheets. By simply controlling the sonication time, FeCl₃-FLG consisting of graphene sheets and sandwiched FeCl₃ is also prepared, which exhibits a high capacity of 989 mAh·g⁻¹ after 50 cycles, fairly higher than that of the sonicated graphite (503 mAh·g⁻¹) and the theoretical value of graphite (372 mAh·g⁻¹). Furthermore, FeCl₃-FLG still retains a reversible capacity as high as 539 mAh·g⁻¹ even at a current density of 1000 mA·g⁻¹. Therefore, the high reversible capacity, remarkable cycling stability and superior capability make FeCl₃-FLG promising as anode materials for large-scale and high-capacity lithium ion batteries.

1. Introduction

Lithium ion batteries (LIBs) are promising in high performance portable electronics and vehicles, which also impose much higher requirement for battery properties.¹ Various carbonaceous and inorganic anode materials are synthesized to enhance the electrochemical performance of LIBs.^{2,3} Compared to commonly utilized graphite, graphene has recently attracted more attention for energy storage and conversion devices due to its large specific surface area, excellent thermal and chemical stability, high electrical and mechanical properties.^{4,5} Various methods including micromechanical exfoliation of graphite,⁶ chemical vapor deposition,⁷ chemically reduction of graphite oxide,^{8,9} bottom-up synthesis from organic compounds,¹⁰ and electrochemical exfoliation,^{11,12} have been developed to prepare graphene and graphene derivatives. Till now, there has been substantial progress in graphene electrode materials for LIBs. Yoo et al. pioneered the research on graphene anode for LIBs and a specific capacity of 540 mAh·g⁻¹ was reported.¹³ The reversible capacity was also improved by enlarging the spacing between graphene sheets. Since then, various graphene anode materials were prepared and the effects of functional groups, specific surface area, interlayer spacing and defects of

graphene were explored.¹⁴⁻¹⁷

It has been confirmed that restacking of graphene sheets would reduce their specific surface area and thus their energy-storage performance.^{3,18} To overcome this problem, many approaches were developed to enlarge the interlayer spacing between graphene sheets and prevent their restacking. Metal oxides anchored on graphene surfaces prevented the aggregation of graphene sheets and exhibited high capacity by synergistic effect of different anode materials.³ Nevertheless, the cyclic stability needs to be improved further. Zhao et al. synthesized un-stacked graphene sheets with as-prepared meso-sized protuberances and used for lithium-sulphur batteries with excellent high-rate performance.¹⁹ Chen et al. fabricated porous α-Fe₂O₃ nanorods supported on three-dimensional (3D) carbon nanotubes-graphene foam, and the highly conductive scaffold with large surface areas afforded the uniform dispersion of the nanorods and thus led to excellent electrochemical performance.²⁰ The intercalation of foreign species is a promising strategy to enhance the interlayer spacing between graphene sheets. Recently, a satisfactory battery capacity was obtained with ferric chloride-graphite intercalation compounds (FeCl₃-GICs) as anode materials for LIBs.^{21,22} However, the large thickness prevented the further improvement of lithium-storage performance. Much thinner few-layer graphene intercalated with FeCl₃ (FeCl₃-FLG) was also prepared based on micromechanically cleaved FLG, which may be difficult for scalable manufacturing, although it exhibited excellent electrical conductivity, charge transport and Fermi level.²³⁻²⁵ Therefore, it is highly desirable to develop a viable and efficient approach for the preparation of FLG with intact structure and high electrical conductivity in

State Key Laboratory of Organic-Inorganic Composites, College of Materials Science and Engineering, Beijing University of Chemical Technology, Beijing 100029, China
Fax: +86-10-64428582; E-mail: zhanghaobin@mail.buct.edu.cn (H.-B. Zhang);
yuzz@mail.buct.edu.cn (Z.-Z. Yu)

† Electronic Supplementary Information (ESI) available: [additional information on elemental analysis, lateral size of specimens, FT-IR spectra and battery properties]. See DOI: 10.1039/b000000x/

spite of the non-oxidation approaches reported for graphene preparation.²⁶⁻²⁹

Herein, FeCl₃-GICs are produced on a large-scale with an intercalation process and used as the precursor to prepare graphene and FeCl₃-FLG by ultrasonication. The enlarged interlayer spacing by the intercalation of FeCl₃ greatly reduces the attraction between adjacent graphene sheets, making it possible for the high-yield production of graphene sheets with a non-oxidation process. Ultrasonic exfoliation of GICs leads to graphene sheets (< 2 nm) with a high yield of 100% and FeCl₃-FLG. FeCl₃-FLG is found to exhibit high reversible capacity, excellent rate capability and cycling stability, indicating its promising potential as anode materials for LIBs.

2. Experimental

2.1 Materials

Natural graphite flakes (300 mesh, 99.9 %) were provided from Huadong Graphite Factory (China) and FeCl₃ (A.R) was obtained from Aladdin (China). N,N-dimethyl formamide (DMF, 99.5%), hydrochloric acid (HCl) and ethanol (99.8%) were bought from Beijing Chemical Factory (China).

2.2 Synthesis and exfoliation of FeCl₃-GICs

FeCl₃ and graphite (w/w, 3/1) were mixed and dried at 120 °C for 6 h, and the mixture was then placed in a stainless-steel autoclave (50 ml) under vacuum at 400 °C for 12 h. To eliminate the detrimental influence of possibly formed iron oxides on exfoliation process, the as-prepared FeCl₃-GICs were rinsed with HCl and deionized water. The synthesized stage 1 FeCl₃-GICs were exfoliated in DMF solvent by ultrasonication for certain time using a JY99-2DN ultrasonicator at 400 W (China). The specimen obtained by ultrasonication of FeCl₃-GICs for 1 h was denoted as FeCl₃-FLG due to its few-layer structure and the intercalated FeCl₃, while ultrasonic exfoliation of FeCl₃-GICs for 6 h results in graphene sheets with negligible residual of FeCl₃. Similar exfoliation process is adopted to exfoliate pristine graphite for control and the resultant is designated as sonicated graphite.

2.3 Characterization

The structure evolution of graphite during intercalation and exfoliation processes was monitored by Rigaku D/Max 2500 X-ray diffraction (XRD) with Cu K α radiation and Renisha winVia Raman microscopy using an excitation wavelength of 514 nm. The compositions of exfoliated GIC, sonicated graphite, and pristine graphite were characterized with ThermoVG RSCAKAB 250X high-resolution X-ray photoelectron spectroscopy (XPS) and Nicolet Nexus 670 Fourier-transform infrared spectroscopy (FT-IR). Morphology observation and energy dispersive analysis (EDS) were carried out on Zeiss Supra 55 field-emission scanning electron microscope (SEM), FEI Tecnai G220 high-resolution transmission electron microscope (TEM), and Bruker multimode 8 atomic force microscope (AFM) under scan Asyst mode. Electrochemical measurement was conducted using specimens as anodes in model CR2025 coin cells. All of the specimens were prepared by spreading a

mixture of active materials, carbon black and polyvinylidene fluoride on Ni foam to prepare the working electrodes. Counter electrode lithium metal foil, separator Celgard 2300 membrane, and electrolyte 1 M LiPF₆ in ethylene carbonate/dimethyl carbonate (1/1, v/v) were assembled with the working electrodes to obtain the half cells in an argon-filled glove-box (OMNI-LAB). The cycle performance of the half cells was evaluated using a LANDCT2001A battery tester. Cyclic voltammetry (CV) measurements were performed using an Autolab PGSTAT 302 N (Metrohm) workstation with a scan rate of 0.1 mV s⁻¹. Electrochemical impedance spectra (EIS) were recorded with the same workstation at amplitude of 10 mV and in the frequency range from 100 KHz to 0.1 Hz.

3. Results and discussion

3.1 Graphene sheets prepared by ultrasonic exfoliation of GICs

Fig. 1 shows the structural changes of graphite after intercalation with FeCl₃. It is clearly seen that natural graphite exhibits ordered structure composed of parallel graphene sheets (Fig. 1a,b). However, after intercalation with FeCl₃, the parallel structure is disrupted and the interlayer spacing is greatly enlarged, leading to an accordion-like structure (Fig. 1c,d). Although the graphene sheets are still partially interconnected with each other, most of them are separated with enlarged interlayer spacing, which would be favourable for them to be exfoliated by sonication. The structure of GICs is determined by stage index. Taking stage 1 GICs for example, each graphene sheet is sandwiched by the intercalated FeCl₃ and the attraction between adjacent graphene sheets is thus weakened. The stage 1 FeCl₃-GICs are promising precursors for the preparation of graphene sheets with intact structure.

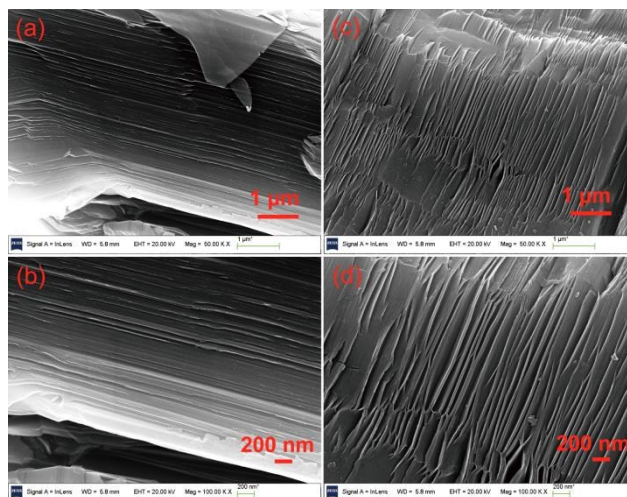


Fig. 1 SEM images of (a,b) natural graphite, and (c,d) stage 1 FeCl₃-GICs under different magnifications.

The influence of intercalated FeCl₃ on exfoliation efficiency of graphite is explored by comparing the thickness of exfoliated products. After ultrasonication for 6 h, the sonicated graphite exhibits obvious multilayer feature (Fig. 2a). In contrast, the graphene sheets resulted from the

ultrasonication of GICs show an ultrathin morphology without notable buckling and ripples (Fig. 2b,c), which are distinct from that of graphene prepared by conventional thermal and chemical reduction of graphite oxide.^{8,9,30} The resultant few-layer structure and quality of as-prepared graphene sheets are further characterized by selected area electron diffraction (SAED) pattern (Inset of Fig. 2c) and Raman spectra. The graphene sheet shown in Fig. 2c is identified as bilayer by its representative high resolution TEM image. Its SAED pattern shows a typical hexagonal symmetry consisting of clear spots with stronger diffraction from (1-210) plane than that from (0-110) plane, indicating the high crystallinity of a bilayer graphene sheet.^{31,32}

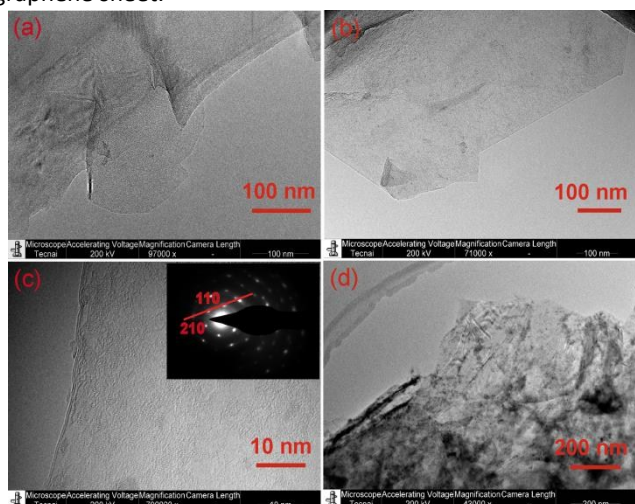


Fig. 2 TEM images of (a) sonicated graphite, (b,c) graphene exfoliated from GICs, and (d) FeCl₃-FLG. The inset of Fig. 2c shows the SAED pattern of graphene.

It is also seen that there are negligible FeCl₃ particles on the surface of graphene sheets, suggesting the nearly complete removal of FeCl₃ from graphene. However, many particles are observed on the slightly thicker graphene sheets of FeCl₃-FLG (Fig. 2d) and these particles are identified as FeCl₃ particles by elemental analysis (Fig. S1). Based on the structure evolution from GICs to graphene sheets, it is confirmed that the anchored FeCl₃ particles are sandwiched between graphene sheets or adsorbed on graphene surface. By simple ultrasonication, stage 1 FeCl₃-GICs are more easily exfoliated to few-layer and even monolayer graphene than pristine graphite. Few-layer graphene sheets intercalated with FeCl₃ are also prepared by controlling the ultrasonication time. This method is more efficient for the preparation of FeCl₃-FLG than that based on the intercalation of mechanically cleaved FLG.⁶ The application of FeCl₃-FLG as new anode material for LIBs is shown below.

To further evaluate the intercalation effect, the thickness of graphene exfoliated from different precursors is determined with AFM and the statistical values are calculated based on 50 flakes (Fig. 3). The thickness of sonicated graphite falls in two distinct thickness ranges, evidenced by different color contrasts (Fig. 3a). Statistical results confirm that 60% of exfoliated flakes have a thickness higher than 5 nm while only

32% of them present a thickness smaller than 2 nm (Fig. 3b). On the contrary, the thickness of graphene prepared the ultrasonication of FeCl₃-GICs falls in a narrow thickness range of 1 to 2 nm. Fig. 3c presents a typical graphene with a thickness of ~1.2 nm, which is close to the average statistical thickness of ~1.22 nm for graphene. Combined with the TEM results, it is confirmed that the resultant graphene contains only two layers of monolayer graphene (Fig. 2c).³²⁻³⁴ Furthermore, the graphene sheets exfoliated from FeCl₃-GICs exhibit a similar mean lateral size (~0.45 μm) to the sonicated graphite (~0.52 μm) (Fig. S2), confirming that the intercalation of graphite with FeCl₃ does not seriously disrupt the flakes. It is clear that the intercalation of FeCl₃ into the intra-gallery of graphite makes it much easier to form bilayer graphene sheets with a high yield. It is noted that mesopores are observed for the graphene sheets exfoliated from FeCl₃-GICs and the sonicated graphite, which may be caused by the sonication process.

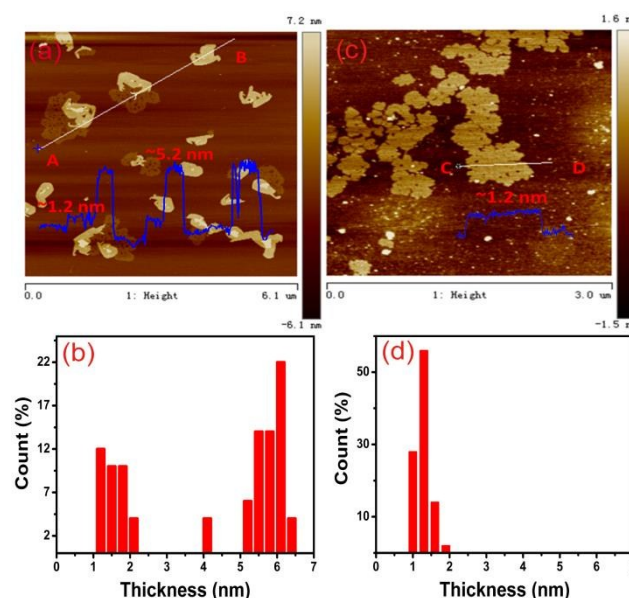


Fig. 3 (a) AFM image of sonicated graphite and (b) its thickness histogram; (c) AFM image of graphene exfoliated from FeCl₃-GICs and (d) its thickness histogram; The height profiles in Fig. 3a and c indicate the thickness.

The stage 1 structure of FeCl₃-GICs is confirmed by XRD (Fig. 4a). Pristine graphite shows a typical XRD pattern with two peaks indexed to (002) and (004), indicating the ordered periodic structure with an interlayer spacing of 0.33 nm. After the intercalation with FeCl₃, new peaks appear at 9.1°, 18.6°, 28.1°, 37.8° and 50.4°, which agrees well with the standard pattern of stage 1 structure of FeCl₃-GICs. However, characteristic peaks of Fe₂O₃ or Fe₃O₄ are not observed in the XRD pattern of FeCl₃-GICs, indicating that even if there are Fe₂O₃ or Fe₃O₄ in GICs, the quantity is too little to be detected by XRD.^{22,35} The d-spacing of FeCl₃-GICs is significantly increased to 0.96 nm from 0.33 nm for graphite. The accordion-like structure is observed in their SEM images (Fig. 1c,d).

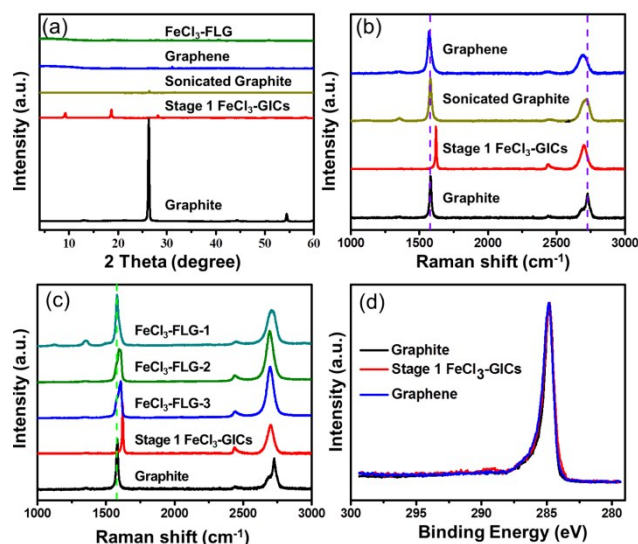


Fig. 4 (a) XRD patterns of pristine graphite, sonicated graphite, graphene, FeCl₃-FLG and stage 1 FeCl₃-GICs; (b) Raman spectra of pristine graphite, sonicated graphite, graphene and stage 1 FeCl₃-GICs; (c) Raman spectra of FeCl₃-FLG with different intercalation extents (FeCl₃-FLG-1, FeCl₃-FLG-2, FeCl₃-FLG-3); (d) XPS spectra of C1s of graphite, graphene, and stage 1 FeCl₃-GICs.

After exfoliation by ultrasonication for 6 h, the resultant graphene sheets exhibit even no noticeable peaks in their XRD pattern, which is consistent with the TEM and AFM results, suggesting their few-layer structure. Similarly, FeCl₃-FLG also indicates a few-layer structure despite the presence of intercalated FeCl₃ particles (Fig. 2d). However, ultrasonication of pristine graphite is less effective in exfoliation, because the resultant still shows a weak peak at 26.4° assigned to (002) plane (Fig. 4a and Fig. S3a).

The structure evolution of graphite during the intercalation with FeCl₃ and the ultrasonic exfoliation is monitored with Raman spectroscopy. The stage structure of FeCl₃-GICs is determined by identifying the component and structure of G peak.^{22,36} Intercalation of FeCl₃ into the intra-gallery of graphite results in a large blue shift for G peak from 1580 to 1621 cm⁻¹, which is attributed to the doping effect induced by the charge transfer from graphite to FeCl₃. Similar results were reported and suggested that graphene sheet is flanked on both sides by FeCl₃ in the stage 1 FeCl₃-GICs.²³⁻²⁵ The 2D-band also exhibits a change from multi-peak structure to single-peak structure, further verifying the loss of electronic coupling between adjacent graphene sheets due to the presence of FeCl₃. However, the G-band of GICs shifts back to 1580 cm⁻¹ after ultrasonication for 6 h and thus the charge transfer between graphite and FeCl₃ disappears. These results are in agreement with the above TEM images and imply the removal of most FeCl₃. Furthermore, the weak D band and low intensity ratio of D/G (< 0.1) for graphene also reflect its less defects.

As recently reported, the intercalated FeCl₃ would contribute to the electrical conductivity of FLG²³ and electrode performance of LIBs.^{21,22} Stage 1 FeCl₃-GICs are used as a promising precursor for the preparation of FeCl₃-FLG by

controlling the exfoliation extent of GICs and the content of retained FeCl₃. Herein, short sonication time of 1 h is used to prepare FeCl₃-FLG and its intercalation homogeneity with FeCl₃ is examined with Raman spectroscopy. Fig. 4c shows Raman spectra of FeCl₃-FLG specimens with different intercalation extents. It is seen that the three specimens have different intercalation stages and concentrations. FeCl₃-FLG-1 presents nearly complete removal of FeCl₃, evidenced by the restored G peak at 1580 cm⁻¹, whereas the G peaks of other two locate at higher wave numbers, which can be deconvoluted to a few peaks, implying the non-uniform intercalation of FeCl₃ in FeCl₃-FLG.⁵ The G-band close to that of stage 2 FeCl₃-GICs and FeCl₃-FLG indicates the presence of graphene sheets flanked on one side by FeCl₃.²³⁻²⁵ The decreased FeCl₃ concentration in FeCl₃-FLG compared to that of its precursor is attributed to the removal of FeCl₃ by ultrasonication. The different locations and shapes of G-band indicate the different intercalation extents of residual FeCl₃. Therefore, this work provides a facile method to prepare graphene and FeCl₃-FLG from GICs by simply adjusting exfoliation time.

The chemical compositions of the graphene, stage 1 FeCl₃-GICs, and graphite are probed with XPS (Fig. 4d). The graphene sheets from GICs exhibit nearly the same C1s spectrum with GICs and graphite, confirming their less defect and intact structure, which is in accordance with the Raman results. However, some oxygen functional groups are introduced during the intercalation of FeCl₃ at 400 °C and subsequent ultrasonication process. By comparing the elemental composition, it is speculated that the oxygen is mainly incorporated in the synthesis of FeCl₃-GICs. This is because graphene is easily oxidized at high temperature and the formation of Fe₂O₃ would also increase the oxygen content of GICs and their derivatives. FT-IR results reveal that the oxygen functionalities on graphene mainly consist of carboxyl groups grafted on the edge of graphene sheets, thus the basal plane of graphene sheets is not seriously affected (Fig. S3b).^{37,38}

3.2 Electrochemical properties of FeCl₃-FLG in LIBs

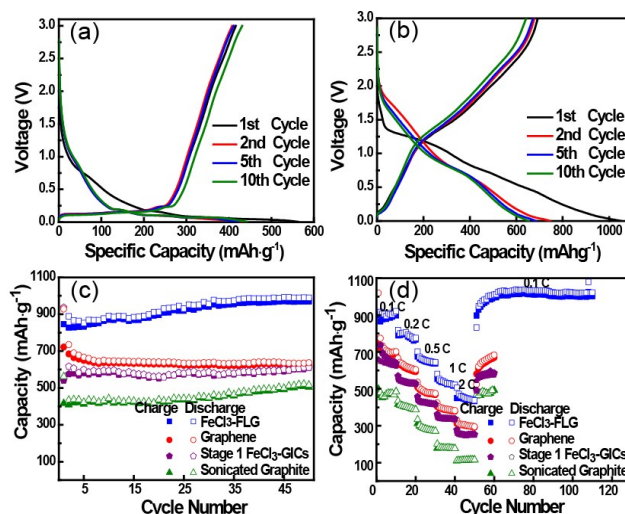


Fig. 5 Charge/discharge curves of (a) sonicated graphite and (b) FeCl₃-FLG between voltage limits of 0.01-3 V at a current of

100 mA·g⁻¹; (c) cycling performance of the specimens at a current density of 100 mA·g⁻¹; (d) rate capabilities of sonicated graphite, stage 1 FeCl₃-GICs, graphene, and FeCl₃-FLG at different rates (100 to 2000 mA·g⁻¹).

Graphene and its derivatives, especially sandwiched-like structured composites, are promising as electrode materials in LIBs.^{2,3,39,40} The electrochemical properties of sonicated graphite, graphene, FeCl₃-FLG, and stage 1 FeCl₃-GICs as anodes in LIBs are evaluated in the potential range of 0.01-3 V at 100 mA·g⁻¹. Fig. 5a and b show the charge/discharge profiles for sonicated graphite and FeCl₃-FLG, respectively. Sonicated graphite presents similar insertion/extraction properties to graphite electrode due to its multilayer structure,^{13,15} while FeCl₃-FLG, graphene and GICs exhibit significantly different charge/discharge profiles, suggesting the different accommodation of lithium ions in these materials from sonicated graphite (Fig. S4).

The discharge curve of FeCl₃-FLG after the initial cycle is divided into two different regions. The capacities of the potential region above 0.25 V are attributed to the formation of LiCl and the reaction of FeCl₃ with Li, while the potential region below 0.25 V may correlate with the lithium intercalation between graphene sheets and Li-ion adsorption/desorption on the FeCl₃ intercalated graphene sheets.^{13,21} The charge/discharge profiles of FeCl₃-FLG anode match well with the shape of the CV curves (Fig. S5). As reported,^{21,22} the electrochemical performance for FeCl₃-GICs and Fe₂O₃/graphite mixture are very similar, redox peaks of both materials are around 0.75V. The reaction mechanism of FeCl₃-FLG could be attributed to the reaction of Fe³⁺ with Li according to the following conversion reaction: FeCl₃ + 3 Li⁺ + 3e⁻ → Fe + 3 LiCl. For Fe₂O₃ based electrodes, the redox peaks are assigned to the highly reversible electrochemical reduction/oxidation (Fe₂O₃ → Fe) reactions.^{20,41} As described in experimental section, intercalation under vacuum and rinse of GICs with HCl solution could greatly avoid or reduce the amount of iron oxide in FeCl₃-GICs. Therefore, the reaction of FeCl₃ with Li mainly contributes to the excellent electrochemical performance of FeCl₃-GIC anode in the present work. In addition, graphene sheets resulted from the exfoliation of FeCl₃-GICs may share the similar mechanism of Li insertion due to the residual FeCl₃ adsorbed on graphene surface, as evidenced by the similar charge/discharge profiles (Fig. S4b).

FeCl₃-GICs could serve as a promising potential anode in LIBs.^{21,22} However, their large size and thickness hinder the transport of lithium ions and electrons, which are crucial for lithium ions storage performance in LIBs. As layered structure with mesopores may facilitate transport of Li-ions, it is envisaged that the graphene sheets resulted from GICs would exhibit a better storage performance of lithium ions. As shown in Fig. 5c, FeCl₃-FLG delivers a discharge capacity of 1378 mAh·g⁻¹ and charge capacity of 845 mA·g⁻¹ in the first cycle, giving an initial coulombic efficiency of 61.3%. The initial irreversible capacity is also observed for other electrode materials, which is ascribed to the electrolyte decomposition

and the solid electrolyte interface film formation on the electrode surface.^{21,22,42} FeCl₃-FLG and graphene sheets exhibit reversible discharge capacities of 989 and 636 mAh·g⁻¹ after 50 cycles, respectively, which are much higher than that of sonicated graphite (503 mAh·g⁻¹) and the theoretical value of pristine graphite (372 mAh·g⁻¹). The stage 1 FeCl₃-GICs show a capability of 610 mAh·g⁻¹, which is consistent with the reported result for stage 1 FeCl₃ intercalated graphite.^{21,22} Therefore, FeCl₃-FLG and graphene are more promising as anode materials than their precursor (FeCl₃-GICs) and the incompletely exfoliated graphite. It is interesting that FeCl₃-FLG exhibits better electrochemical performance than graphene despite the thinner characteristic of the latter, which may be due to the residual FeCl₃ in FeCl₃-FLG as the main active material.

The cyclic stability of FeCl₃-FLG and other specimens is investigated at different current densities from 100 to 2000 mA·g⁻¹. Because of such a thin and porous structure, FeCl₃-FLG demonstrates the best rate performance among the specimens. FeCl₃-FLG and graphene sheets show specific capabilities of 539 and 394 mAh·g⁻¹ even at 1000 mA·g⁻¹, respectively, which are pretty higher than that of sonicated graphite (182 mAh·g⁻¹) (Fig. 5d). Even at current density of as high as 2000 mA·g⁻¹, FeCl₃-FLG still retains a specific capability of 362 mAh·g⁻¹. Such an excellent rate performance is better than both graphene and FeCl₃-GICs. In contrast, the capacity of stage 1 FeCl₃-GICs is decreased to 255 mAh·g⁻¹, 1.8 times lower than that of FeCl₃-FLG at current density of 2000 mA·g⁻¹. Li-ions could rapidly insert/extract into the intra-gallery to react with FeCl₃ during cycling due to the nanoscale thickness and porous structure of FeCl₃-FLG. Therefore, FeCl₃-FLG exhibits a better rate performance than stage 1 FeCl₃-GICs, especially at high current densities. After rate cycling, FeCl₃-FLG still presents an excellent reversible capacity of 1002 mAh·g⁻¹ at 100 mA·g⁻¹ for another 60 cycles, fairly higher than those of stage 1 FeCl₃-GICs and sonicated graphite. Such a high reversible capacity is one of the highest values for graphene anode in LIBs.^{3,13,15-17,21,22} Even the graphene sheets also exhibit a significant increase in capacity in relative to sonicated graphite and comparable properties to graphene anodes.^{27,43} Therefore, higher cyclic capability and better cycling stability are achieved by using FeCl₃-FLG as the anode material for LIBs as compared to other graphene anode materials.^{14,15,17-19}

The remarkable capability and excellent cycling stability of FeCl₃-FLG can be attributed to its robust and unique structures. Firstly, the few-layer structure of FeCl₃-FLG contributes to the battery properties by providing buffer matrix for the volume change of FeCl₃ during lithiation/delithiation.^{21,22} Secondly, the intercalated FeCl₃ greatly enlarges the interlayer spacing of graphite and thus provides additional sites for the accommodation of Li-ions. After sonication treatment, the interlayer spacing is further enlarged and mesopores are also formed on the surfaces of the as-prepared specimen, both of them provide convenient channels for the rapid insertion/extraction of Li-ions during the electrode reaction. The influence of enhanced interlayer spacing on the anode performance has been confirmed in different anode

materials.^{14,17,39,40,44} Thirdly, the intercalation of FeCl₃ improves the electrical conductivity of pristine graphite to get a better electrochemical performance.^{14,21,22,35,45} The higher electrical conductivity of FeCl₃-FLG is verified by the obviously reduced diameter of the semicircle at the high-frequency region in the electrochemical impedance spectrum (Fig. S6).^{22,45,46} As reported,²¹ both thicker FLG (< 5 layers) and FeCl₃-FLG usually present higher electrical conductivity than their thinner counterparts. Therefore, stage 1 FeCl₃-GICs exhibit much lower capacity than FeCl₃-FLG despite its higher concentration of intercalated FeCl₃.

Conclusions

Graphene and FeCl₃-FLG are prepared by ultrasonication of stage 1 FeCl₃-GICs and both of them exhibit reversible discharge capacities of 636 and 989 mAh·g⁻¹ after 50 cycles, respectively, much higher than that of sonicated graphite (503 mAh·g⁻¹). Moreover, FeCl₃-FLG still retains a reversible capacity as high as 1002 mAh·g⁻¹ even after 110 cycles. The excellent battery performance of FeCl₃-FLG is attributed to the buffer matrix provided by few-layer structure, increased interlayer spacing, and improved electrical conductivity. The high reversible capacity, remarkable cycling stability, and superior capability suggest that FeCl₃-FLG holds a huge promise as anode material for high performance LIBs.

Acknowledgements

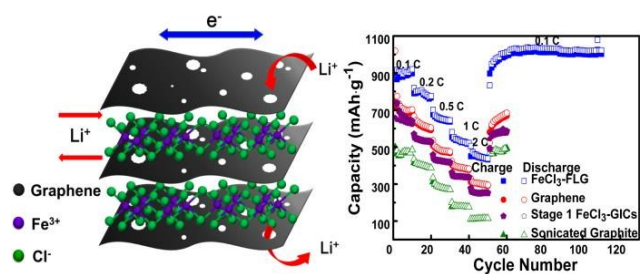
Financial support from the National Natural Science Foundation of China (51373011, 51103007, 51125010) is gratefully acknowledged.

Notes and references

- 1 M. Armand and J. M. Tarascon, *Nature*, 2008, **451**, 652-657.
- 2 D. S. Su and R. Schlögl, *ChemSusChem*, 2010, **3**, 136-168.
- 3 Z. S. Wu, G. Zhou, L. C. Yin, W. Ren, F. Li and H. M. Cheng, *Nano Energy*, 2012, **1**, 107-131.
- 4 K. S. Novoselov, V. I. Falko, L. Colombo, P. R. Gellert, M. G. Schwab and K. Kim, *Nature*, 2012, **490**, 192-200.
- 5 L. Liu, S. Ryu, M. R. Tomasik, E. Stolyarova, N. Jung, M. S. Hybertsen, M. L. Steigerwald, L. E. Brus and G. W. Flynn, *Nano Lett.*, 2008, **8**, 1965-1970.
- 6 K. S. Novoselov, A. K. Geim, S. V. Morozov, D. Jiang, Y. Zhang, S. V. Dubonos, I. V. Grigorieva and A. A. Firsov, *Science*, 2004, **306**, 666-669.
- 7 K. S. Kim, Y. Zhao, H. Jang, S. Y. Lee, J. M. Kim, K. S. Kim, J. H. Ahn, P. Kim, J. Y. Choi and B. H. Hong, *Nature*, 2009, **457**, 706-710.
- 8 H. B. Zhang, J. W. Wang, Q. Yan, W. G. Zheng, C. Chen and Z. Z. Yu, *J. Mater. Chem.*, 2011, **21**, 5392-5397.
- 9 H. B. Zhang, W. G. Zheng, Q. Yan, Z. G. Jiang and Z. Z. Yu, *Carbon*, 2012, **50**, 5117-5125.
- 10 X. Y. Yang, X. Dou, A. Rouhanipour, L. J. Zhi, H. J. Räder and K. Müllen, *J. Am. Chem. Soc.*, 2008, **130**, 4216-4217.
- 11 J. L. Liu, C. k. Poh, D. Zhan, L. F. Lai, S. H. Lim, L. Wang, X. X. Lina, N. G. Sahoo, C. M. Li, Z. X. Shen and J. Y. Lin, *Nano Energy*, 2013, **2**, 377-386.
- 12 J. L. Liu, H. P. Yang, S. G. Zhen, C. k. Poh, A. Chaurasia, J. S. Luo, X. Y. Wu, E. K. L. Yeow, N. G. Sahoo, J. Y. Lin and Z. X. Shen, *RSC Adv*, 2013, **3**, 11745-11750.
- 13 E. Yoo, J. Kim, E. Hosono, H. S. Zhou, T. Kudo and I. Honma, *Nano Lett.*, 2008, **8**, 2277-2282.
- 14 G. Wang, X. Shen and J. Yao, *Carbon*, 2009, **47**, 2049-2053.
- 15 P. Guo, H. Song and X. Chen, *Electrochem. Commun.*, 2009, **11**, 1320-1324.
- 16 P. Lian, X. Zhu and S. Liang, *Electrochim. Acta*, 2010, **55**, 3909-3914.
- 17 D. Pan, S. Wang, B. Zhao, M. Wu, H. Zhang, Y. Wang and Z. Jiao, *Chem. Mater.*, 2009, **21**, 3136-3142.
- 18 C. Wang, D. Li, C. O. Too and G. G. Wallace, *Chem. Mater.*, 2009, **21**, 2604-2606.
- 19 M. Q. Zhao, Q. Zhang, J. Q. Huang, G. L. Tian, J. Q. Nie, H. J. Peng and F. Wei, *Nat. Commun.*, 2014, **5**, 3410.
- 20 M. H. Chen, J. L. Liu, D. L. Chao, J. Wang, J. H. Yin, J. Y. Lin, H. J. Fan and Z. X. Shen, *Nano Energy*, 2014, **9**, 364-372.
- 21 F. Wang, J. Yi, Y. Wang, C. Wang, J. Wang and Y. Xia, *Adv. Energy Mater.*, 2014, **4**, 1300600.
- 22 L. Wang, Y. Zhu, C. Guo, X. Zhu, J. Liang and Y. Qian, *ChemSusChem*, 2014, **7**, 87-91.
- 23 I. Khrapach, F. Withers, T. H. Bointon, D. K. Polyushkin, W. L. Barnes, S. Russo and M. F. Craciun, *Adv. Mater.*, 2012, **24**, 2844-2849.
- 24 D. Zhan, L. Sun, Z. H. Ni, L. Liu, X. F. Fan, Y. Wang, T. Yu, Y. M. Lam, W. Huang and Z. X. Shen, *Adv. Funct. Mater.*, 2010, **20**, 3504-3509.
- 25 W. Zhao, P. H. Tan, J. Liu and A. C. Ferrari, *J. Am. Chem. Soc.*, 2011, **133**, 5941-5946.
- 26 C. J. Shih, A. Vijayaraghavan, R. Krishnan, R. Sharma, J. H. Han, M. H. Ham, Z. Jin, S. Lin, G. L. C. Paulus, N. F. Reuel, Q. H. Wang, D. Blankschtein and M. S. Strano, *Nat. Nanotechnol.*, 2011, **6**, 439-445.
- 27 X. Geng, Y. Guo, D. Li, W. Li, C. Zhu, X. Wei, M. Chen, S. Gao, S. Qiu, Y. Gong, L. Wu, M. Long, M. Sun, G. Pan and L. Liu, *Sci. Rep.*, 2013, **3**, 1134.
- 28 J. N. Coleman, M. Lotya, A. O'Neill, S. D. Bergin, P. J. King, U. Khan, K. Young, A. Gaucher, S. De and R. J. Smith, *Science*, 2011, **331**, 568-571.
- 29 M. Ujihara, M. M. Mahmoud Ahmed, T. Imae and Y. Yamauchi, *J. Mater. Chem. A*, 2014, **2**, 4244-4250.
- 30 S. Stankovich, D. A. Dikin, G. H. B. Dommett, K. M. Kohlhaas, E. J. Zimney, E. A. Stach, R. D. Piner, S. T. Nguyen and R. S. Ruoff, *Nature*, 2006, **442**, 282-286.
- 31 Y. Hernandez, V. Nicolosi, M. Lotya, F. M. Blighe, Z. Sun, S. De, I. T. McGovern, B. Holland and M. Byrne, *Nat. Nanotechnol.*, 2008, **3**, 563-568.
- 32 K. Parvez, Z. S. Wu, R. Li, X. Liu, R. Graf, X. Feng and K. Müllen, *J. Am. Chem. Soc.*, 2014, **136**, 6083-6091.
- 33 Z. Cheng, Q. Zhou, C. Wang, Q. Li, C. Wang and Y. Fang, *Nano Lett.*, 2011, **11**, 767-771.
- 34 M. J. McAllister, J. L. Li, D. H. Adamson, H. C. Schniepp, A. A. Abdala, J. Liu, M. Herrera-Alonso, D. L. Milius, R. Car, R. K. Prud'homme and I. A. Aksay, *Chem. Mater.*, 2007, **19**, 4396-4404.
- 35 M. S. Dresselhaus and G. Dresselhaus, *Adv. Phys.*, 2002, **51**, 1-186.
- 36 A. M. Dimiev, G. Ceriotti, N. Behabtu, D. Zakhidov, M. Pasquali, R. Saito and J. M. Tour, *ACS Nano*, 2013, **7**, 2773-2780.
- 37 I. Y. Jeon, Y. R. Shin, G. J. Sohn, H. J. Choi, S. Y. Bae, J. Mahmood, S. M. Jung, J. M. Seo, M. J. Kim, D. Wook Chang, L. Dai and J. B. Baek, *Proc. Natl. Acad. Sci.*, 2012, **109**, 5588-5593.
- 38 D. R. Dreyer, S. Park, C. W. Bielawski and R. S. Ruoff, *Chem. Soc. Rev.*, 2010, **39**, 228-240.

- 39 J. Qu, Y. X. Yin, Y. Q. Wang, Y. Yan, Y. G. Guo and W. G. Song, *ACS Appl. Mater. Interfaces*, 2013, **5**, 3932-3936.
- 40 J. Qu, Y. Yan, Y. X. Yin, Y. G. Guo and W. G. Song, *ACS Appl. Mater. Interfaces*, 2013, **5**, 5777-5782.
- 41 J. L. Liu, W. W. Zhou, L. F. Lai, H. P. Yang, S. H. Lim, Y. D. Zhen, T. Yu, Z. X. Shen and J. Y. Lin, *Nano Energy*, 2013, **2**, 726-732.
- 42 N. A. Kaskhedikar and J. Maier, *Adv. Mater.*, 2009, **21**, 2664-2680.
- 43 M. Liang and L. Zhi, *J. Mater. Chem.*, 2009, **19**, 5871-5878.
- 44 S. Yata, H. Kinoshita, M. Komori, N. Ando, T. Kashiwamura, T. Harada, K. Tanaka and T. Yamabe, *Synth. Met.*, 1994, **62**, 153-158.
- 45 Z. S. Wu, W. Ren, L. Xu, F. Li and H. M. Cheng, *ACS Nano*, 2011, **5**, 5463-5471.
- 46 K. Chang and W. Chen, *J. Mater. Chem.*, 2011, **21**, 17175-17184.

Table of Contents



$\text{FeCl}_3\text{-FLG}$ prepared from graphite intercalation compounds exhibits a reversible capacity as high as $1002 \text{ mAh}\cdot\text{g}^{-1}$ even after 110 cycles.